LABPLAS

Horizon 2020
European Union Funding
for Research & Innovation

Land-Based Solutions for Plastics in the Sea

This project has received funding from the European Union's Horizon 2020 research and innovation programme under grant agreement No 101003954

D4.4 Final Report on SMNPs presence in the analysed field samples

Due date of deliverable: 30/11/2024

Actual submission date: 29/11/2024

Horizon 2020
European Union Funding
for Research & Innovation

LABPLAS

Horizon 2020
European Union Funding
for Research & Innovation

PROJECT INFORMATION

Project number: 101003954

Project acronym: LABPLAS

Project full title: Land-Based Solutions for Plastics in the Sea

Call: H2020-SC5-2018-2019-2020 submitted for H2020-SC5-2020-2 / 03 Sep 2020

Topic: CE-SC5-30-2020 – Plastics in the environment: understanding the sources, transport, distribution and impacts of plastics pollution

Type of action: RIA – Research and Innovation Action

Starting date: June 1st, 2021

Duration: 48 months

List of participants:

Nº	Participant name	Acronym	Country	Type
1	UNIVERSIDADE DE VIGO	UVI	SPAIN	HES
2	UNIVERSIDADE DA CORUÑA	UDC	SPAIN	HES
3	Bundesanstalt fuer Gewaesserkunde	BfG	GERMANY	RTO
4	LABORATORIO IBERICO INTERNACIONAL DE NANOTECNOLOGIA	INL	PORTUGAL	RTO
5	KATHOLIEKE UNIVERSITEIT LEUVEN	KUL	BELGIUM	HES
6	HELMHOLTZ ZENTRUM FUR OZEANFORSCHUNG KIEL	GEOMAR	GERMANY	RTO
7	NATIONAL OCEANOGRAPHY CENTRE	NOC	UNITED KINGDOM	RTO
8	SORBONNE UNIVERSITE	SU	FRANCE	HES
9	OPEN UNIVERSITEIT NEDERLAND	OUNL	NETHERLANDS	HES
10	LEIBNIZ INSTITUTE FOR BALTIC SEA RESEARCH	IOW	GERMANY	RTO
11	ASSOCIACAO PARA O DESENVOLVIMENTO DO ATLANTIC INTERNATIONAL RESEARCH CENTRE	AC	PORTUGAL	RTO
12	UNIVERSIDADE FEDERAL DE SAO PAULO	UNIFESP	BRAZIL	HES
13	BASF SE	BASF	GERMANY	LE
14	TG ENVIRONMENTAL RESEARCH	ER	UNITED KINGDOM	SME
15	CONTACTICA S.L.	CTA	SPAIN	SME
16	STICHTING EGI	EGI	NETHERLANDS	Non-P
17	STICHTING RADBOUD UNIVERSITEIT	RU	NETHERLANDS	HES
18	UNIVERSIDADE FEDERAL DO PARÁ	UFPA	BRAZIL	HES

DELIVERABLE DETAILS

Document Number:	D4.4
Document Title:	Final Report on SMNPs' presence in the analysed field samples
Dissemination level	PU – Public
Period:	PR3
WP:	WP4
Task:	Task 4.3
Status:	Final
Author:	INL INTERNATIONAL IBERIAN NANOTECHNOLOGY LABORATORY; UNIVERSIDADE DA CORUÑA
Reviewers:	UNIVERSIDADE DA CORUÑA
Recommended citation format	2024. Final Report on SMNPs presence in the analysed field samples. Deliverable 4.4, LABPLAS Grant Agreement No. 101003954 H2020-SC5-2020-2
Abstract:	We report the analysis of SMNPs from field samples collected during LAPBLAS sampling campaigns (WP2, D2.2 and D2.3). Water samples from the Elbe, Thames, Mero-Barcés and the North Sea and suspended sediments from water samples from Mero-Barcés, Elbe, and Thames were processed and analysed following the guidelines presented in Deliverable 4.1, Guideline for methods for extraction, pre-concentration and purification of SMNPs. The results shown in this Deliverable 4.4 were generated in the framework of LABPLAS Task 4.3. This report describes the analysis carried out by Raman and Py-GC-MS. Raman analysis after accumulating and size-sorting the smallest small microplastics in the Lab-on-a-chip developed in Task 4.2 was performed, and the results are also reported in this deliverable.

Version	Date	Comments
1.0	29.11.2024	Final Report on SMNPs presence in the analysed field samples.
2.0	14.07.2025	Reviewed with changes to address comments by the PO and reviewer.

Disclaimer

The views and opinions expressed in this document reflect only the authors' views, and not necessarily those of the European Commission.

TABLE OF CONTENTS

LIST OF FIGURES

LIST OF TABLES

ABBREVIATIONS AND ACRONYMS

Abbreviation / Acronym	Description
ABS	Acrylonitrile Butadiene Styrene copolymer
CPE	Cloud Point Extraction
D	Deliverable
DiO	3,3′-DiOctadecyloxacarbocyanine perchlorate
NIST	National Institute of Standards and Technology
NTA	Nanoparticle Tracking Analysis
PA 6	Nylon-6
PA 6,6	Nylon-6,6
PC	Polycarbonate
PE	Polyethylene
PET	Polyethylene terephthalate
PMMA	Polymethyl methacrylate
PP	Polypropylene
PS	Polystyrene
PVC	Polyvinylchloride
Py-GC-MS	Pyrolysis Gas Chromatography coupled to Mass Spectrometry
SBR	Styrene-butadiene rubber
SERS	Surface-Enhanced Raman Scattering
SMNPs	Small, Micro- and Nanoplastics
SRMs	Standard Reference Materials
WP	Work Package

1 INTRODUCTION

Currently, the detection and identification of the smallest small microplastics (<10 µm – 1000 nm) and nanoplastics (1000 nm – 1 nm) (SMNPs) in environmentally relevant samples is highly challenging because of the lack of standardized analytical procedures.

The Commission Delegated Decision Supplementing Directive (EU) 2020/2184 of the European Parliament and the Council, by laying down a methodology to measure microplastics in water intended for human consumption, established that the compositional analysis of microplastic particles and fibres shall be carried out using vibrational spectroscopy methods such as Fourier-Transform IR micro-spectroscopy (µ-FTIR), Raman micro-spectroscopy (µ-Raman) or equivalent variations. µFTIR presents a theoretical size limit of ~5.0 µm (although 10 µm is the actual acknowledged limit) and µRaman, 1.0 µm. Furthermore, recent studies have shown that the 1–10 µm MP may represent most of the MP population in the drinking water samples (Maurizi et al., 2023). As the scope of the study in this deliverable is SMNPs (<10 µm), we chose µ-Raman and Raman spectroscopy coupled to microfluidics for the analysis of this size fraction in LABPLAS samples.

This deliverable describes the analysis of the field samples of water and suspended sediments collected during the sampling campaigns (D2.2 and D2.3) to determine the presence of SMNPs. This analysis was carried out following the guidelines described in D4.1. The results of suspended sediments reported here are based on the analysis of the samples after density separation and filtration using Raman spectroscopy. The results of water samples included in the deliverable are based on the analysis of the samples using Raman spectroscopy and Py-GC-MS after CPE and filtration purification. These water samples were also analysed using the Lab-on-a-chip system developed for the smallest small microplastics, allowing the study of its performance compared with the results obtained with the standard protocol.

2 SUSPENDED SEDIMENTS ANALYSIS

As described in Deliverable 4.3, suspended sediments were observed in:

- MB4-03-BO-06-01 (i.e., MB4-Meirame sampled in the Spring campaign)
- All samples from the Thames River: T03-Windsor (upstream of tidal limit) at two depths: surface and 1 m, T05-Central London (urban), and T06-Thames estuary (Chapman Buoy).
- All samples from the Elbe River: E14-Hamburg at different depths: 10 cm (surface), 50 and 200 cm, E15-Geesthacht, E16-Dömitz, and E17-Dessau.

Suspended sediments were then isolated and separated by density following the procedure described in D4.1 and D4.3. It is worth noting that the final quantity of sediments isolated from the water was very small, so the weights could not be registered. We used a set of filters in the final step of separation: 80 µm Nylon membrane, 0.7 µm glass fiber membrane and 0.1 µm anodisc. Both nylon and glass fiber membranes contained few particles (< 30 particles per filter) observable with a confocal Raman microscope (≥ 1 µm). The highest number of particles per filter, 28 particles/fibers, was found in the glass fiber membrane of the E15-Geesthacht sample, as shown in Figure 1.

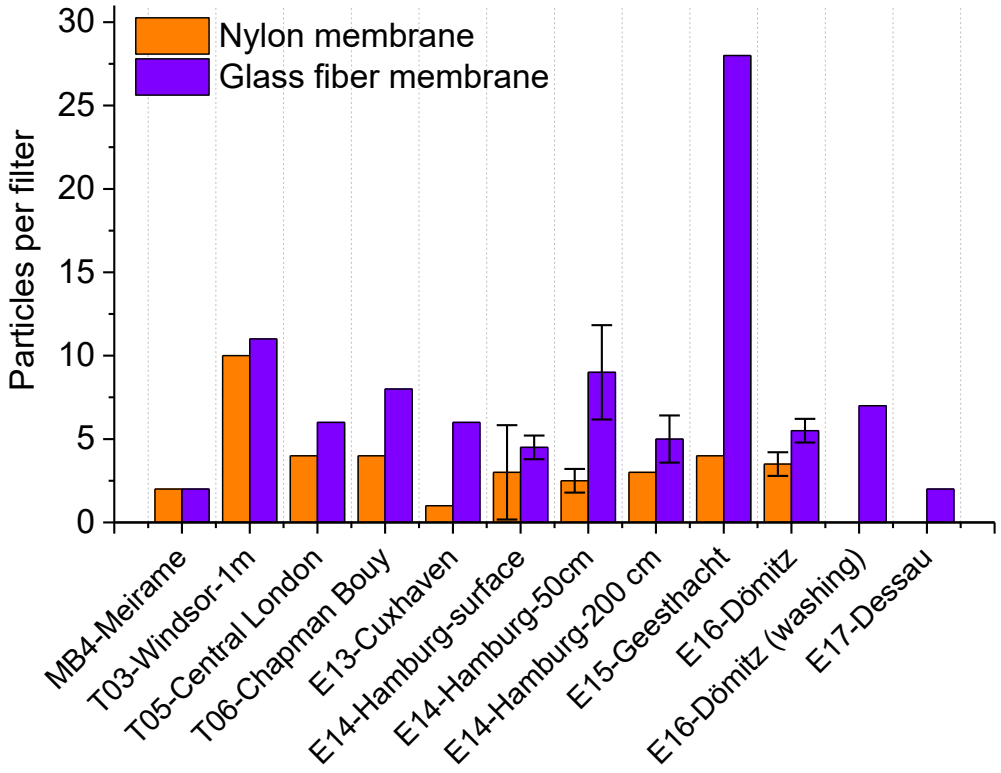

Figure 1. Estimation of the number of particles collected in the 80 µm nylon membrane and 0.7 µm glass fiber membrane by filtering the supernatant from the density separation procedure.

The number of particles on 0.1 µm anodisc was not estimated mainly for two reasons: 1) There would be an underestimation of the number due to the size: all particles (or aggregates) are smaller than 0.7 µm at least in one of the dimensions and many of them are outside of the spatial resolution of the confocal Raman microscopy

(around 1 µm[1]), and 2) The release of several fibers from the glass membrane used previously (see bright-field images of anodisc in Figure 6), provoking an overestimation of the number of particles present in the anodisc.

Next, we analyzed stained particles using fluorescence microscopy. Nile Red must be avoided in the case of suspended sediments since the particulate matter displays auto-fluorescence in the same spectral range as Nile Red (559 nm excitation, 635 nm emission)[2, 3] interfering with the fluorescence analysis of the particles. Therefore, the suspended sediments were stained from the beginning of the sample preparation using DiO as described in D4.1 and D4.3, allowing the direct visualization of particles on each membrane using a fluorescence microscope. Samples were imaged using an objective of at least 40× and the DiO imaging optimal conditions (483 nm excitation, 501 nm emission). The analysis by fluorescence microscopy was described in Deliverable 4.3 and summarized here:

- MB4-03-BO-06-01: Few fluorescent particles with spherical shape and a size close to 10 µm.
- T03-Windsor sampled at 1 m depth: many particles with irregular shape.
- T03-Windsor sampled on the surface: some small and roundish particles.
- T05-Central London and T06-Chapman buoy: bigger particles and in smaller quantities than the T03 samples.
- E13-Cuxhaven: smaller particles than the rest of the Elbe River samples, and some of them showed sizes smaller than 1 µm.
- E14-Hamb, E15-Geesthacht, E16-Dömitz, and E17-Dessau: Few fluorescent particles with irregular shapes and sizes, bigger than in E13.

After a visualization by optical microscopy and fluorescence analysis of DiO-stained particles, we performed the identification of the particles and/or fibers accumulated in the three membranes. In the case of the analysis of 0.1 µm anodisc, we focused on the pre-localized fluorescent particles to reduce the time of analysis.

2.1 Py-GC-MS

Due to the limited quantity of suspended sediments, we could perform the whole procedure once. Therefore, we characterized samples first with microRaman since this is a non-destructive technique. We sent the filters to UDC once the Raman analysis was finished to carry out Py-GC-MS measurements since it is a destructive technique.

2.2 Raman identification

The Raman measurement conditions for stained suspended sediments using a Raman confocal microscope (300 lines mm^{-1} grating and a CCD camera) were slightly modified due to spectral interference of DiO[4], as described in D4.3. Therefore, the spectra should be acquired using a 785 nm laser line with a laser power $\geq$ 4 mW and objectives of 20× and 50×. 633 nm laser line could not be used for these kinds of samples due to the high fluorescence background coming from the rest of the particles present in the matrix (e.g. particulate

[1] Xu, J.-L., Thomas, K.V., Luo, Z., Gowen, A.A., FTIR and Raman imaging for microplastics analysis: State of the art, challenges and prospects. TrAC Trends in Analytical Chemistry 2019. **119**.

[2] Cottrell BA, Timko SA, Devera L, Robinson AK, Gonsior M, Vizenor AE, et al. Photochemistry of excited-state species in natural waters: A role for particulate organic matter. Water Research 2013, **47**.

[3] Cabrera-Brufau M, Marrasé C, Ortega-Retuerta E, Nunes S, Estrada M, Sala MM, et al. Particulate and dissolved fluorescent organic matter fractionation and composition: Abiotic and ecological controls in the Southern Ocean. Science of the Total Environment 2022, **844**.

[4] Feng G, Suzuki N, Zhang Q, Li J, Inose T, Taemaitree F, et al. A light-mediated covalently patterned graphene substrate for graphene-enhanced Raman scattering (GERS). Chemical Communications 2023, **59**

organic matter[5] [6]). It is worth noting that all PE peaks in the spectral window of 1000 – 2000 cm^{-1} overlapped with the DiO spectra. Consequently, the identification of PE stained with DiO using a 785 nm laser line was limited to cases when DiO staining was low (see more details in D4.3).

As commented above, we focused on the DiO-stained particles, which presented an orange colour when visualizing with a confocal Raman microscope. They were visualized easily in 80 µm nylon and 0.7 µm glass fiber membranes because particles were bigger than in anodics, as expected. For particles' localization in anodics, we pre-visualized them by fluorescence microscopy and then, we performed the Raman analysis in these pre-localized particles. Almost all samples contained some DiO-stained particles, except suspended sediments collected from MB4-03-BO-06-01, E17-Dessau, T03-Windsor water sampled at 1 m and E16-Dömitz – washing.

As expected, stained particles observed in both nylon and glass fiber membranes displayed Raman fingerprints involving characteristic peaks of DiO dye, which made it more difficult to identify the particle nature. Additionally, almost all Raman spectra showed a fluorescence background. Several stained particles could not be identified by Raman due to the high interference from the DiO fingerprint in the vibrational spectrum of the particle, which means that none or only a few peaks could be differentiated from the characteristic peaks of DiO (Figure 2). Furthermore, the peaks that were not assigned to DiO did not correspond to any of the plastics included in the database generated for SMNPs in WP4, e.g. PS, PET, PE, and PP.

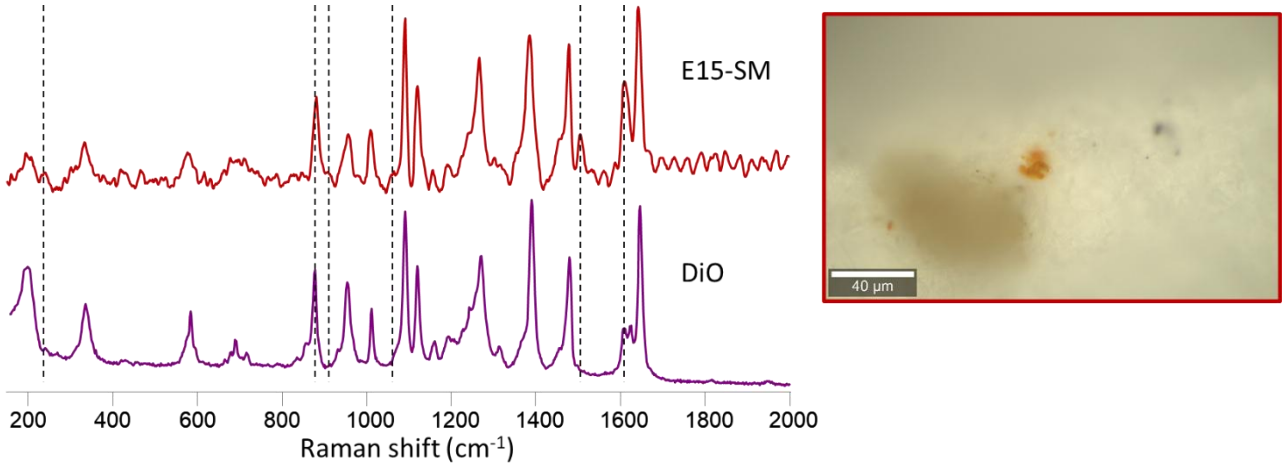

Figure 2. Raman spectra of DiO dye (purple) and stained particle from suspended sediments of E15-Geesthacht water sampled in the surface microlayer and collected on a glass fiber membrane. All spectra were processed by correcting the baseline, removing cosmic rays, and normalizing. Back dashed lines indicate the peaks that do not correspond to the DiO fingerprint in the Raman spectrum of stained particle from E15-Geesthacht suspended sediments. A representative bright image, which shows the shape and size of the particles analyzed.

For several particles found in the membranes, several peaks could be differentiated from DiO characteristic peaks, as shown in Figure 3. However, none of these peaks corresponded to PS, PET, PP, or PE. We could not assign those peaks to any molecule despite using a Raman library of microplastics (STJ Spectral Databases).

[5] Cottrell BA, Timko SA, Devera L, Robinson AK, Gonsior M, Vizenor AE, et al. Photochemistry of excited-state species in natural waters: A role for particulate organic matter. Water Research 2013, **47**.

[6] Cabrera-Brufau M, Marrasé C, Ortega-Retuerta E, Nunes S, Estrada M, Sala MM, et al. Particulate and dissolved fluorescent organic matter fractionation and composition: Abiotic and ecological controls in the Southern Ocean. Science of the Total Environment 2022, **844**.

The Raman fingerprints shown in Figure 3 were acquired in particles collected from the T06-Chapman buoy, T05-Central London, E16-Dömitz, E15-Geesthacht, E14-Hamburg, and E13-Cuxhaven.

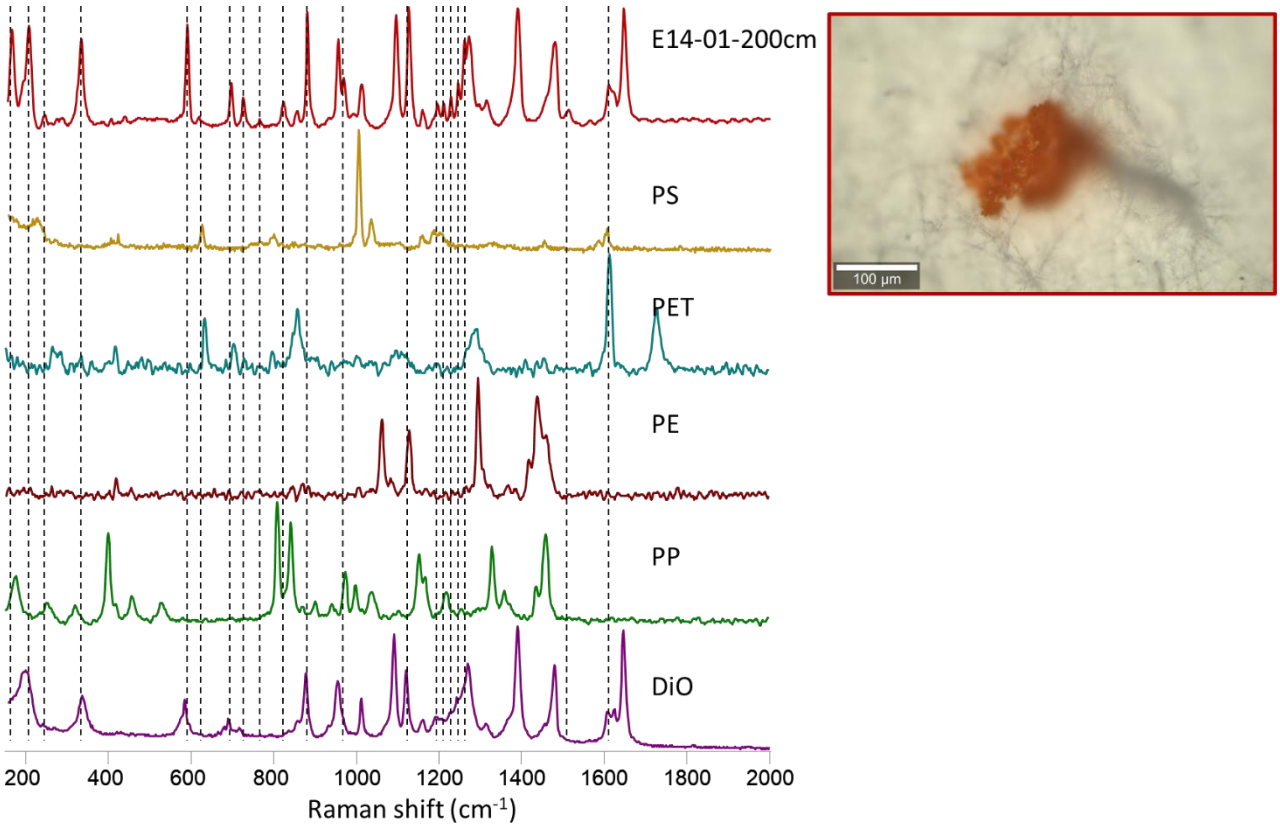

Figure 3. Raman spectra of DiO dye (purple), unstained microplastics made from PP (green), PE (wine red), PET (cyan), and PS (yellow), and stained particle from suspended sediments of E14-Hamburg water sampled at 200 cm depth and collected on a glass fiber membrane. All spectra were processed by correcting the baseline, removing cosmic rays, and normalizing. Back dashed lines indicate the peaks that do not correspond to the DiO fingerprint in the Raman spectrum of stained particle from E14-Hamburg suspended sediments. A representative bright image, which shows the shape and size of the particles analyzed.

After analyzing the DiO-stained particles, we performed the characterization of unstained particles. Interestingly, we identified PP in T03-Windsor water sampled at 1 m (Figure 4), E14-Hamburg at 50 cm depth (bottle 2; Figure 5) and T06-Chapman buoy (Figure 6), PE in E14-Hamburg at 50 cm depth (bottle 1; Figure 5), and PS in E15-Geesthacht and MB4-03-BO-06-01 (Figure 6). All particles/fibers had a size in the micro-scale, except the PS particle in MB4-03-BO-06-01, which is close to 1 µm. It is worth noting that PP and PE were detected in the same sampling point, but in different sampling replicates (PE was detected in bottle 1 and PP in bottle 2). This may have an impact on the sampling procedure for SMNPs, having to collect a higher volume of sample to have enough quantity of suspended sediments to carry out this kind of analysis.

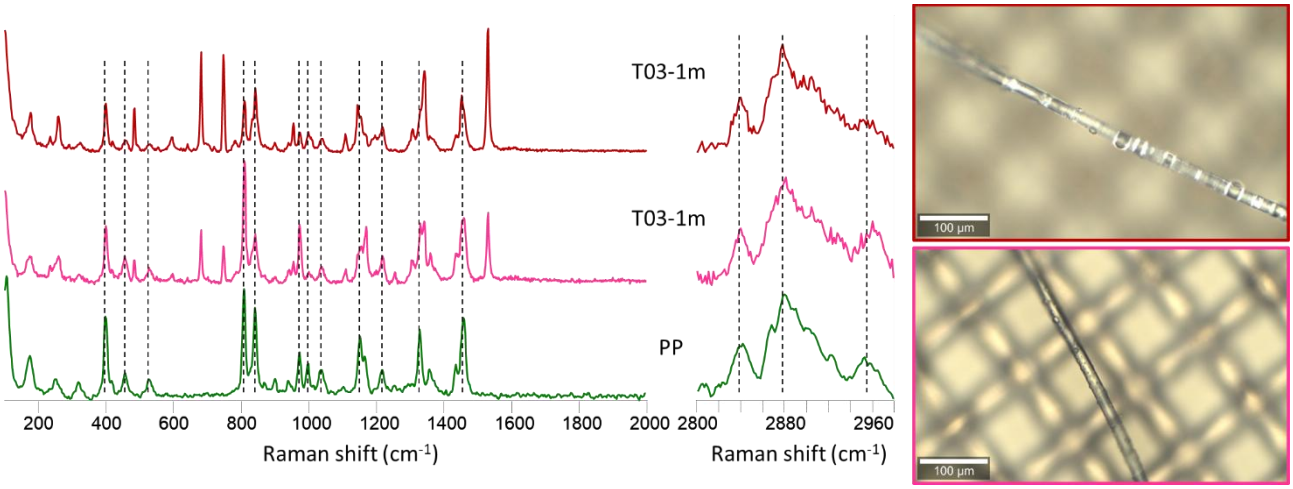

Figure 4. Raman spectra of fibers collected from suspended sediments of T03-Windsor water sampled at 1 m depth. The fibers were visualized in the nylon membrane. The Raman spectrum of micronized PP was included as a reference, demonstrating that the fibers are made from this polymer. All spectra were processed by correcting the baseline, removing cosmic rays, and normalizing. Back dashed lines indicate the peaks assigned to PP. Bright images show the shape and size of the particles (in this case, fibers) analyzed.

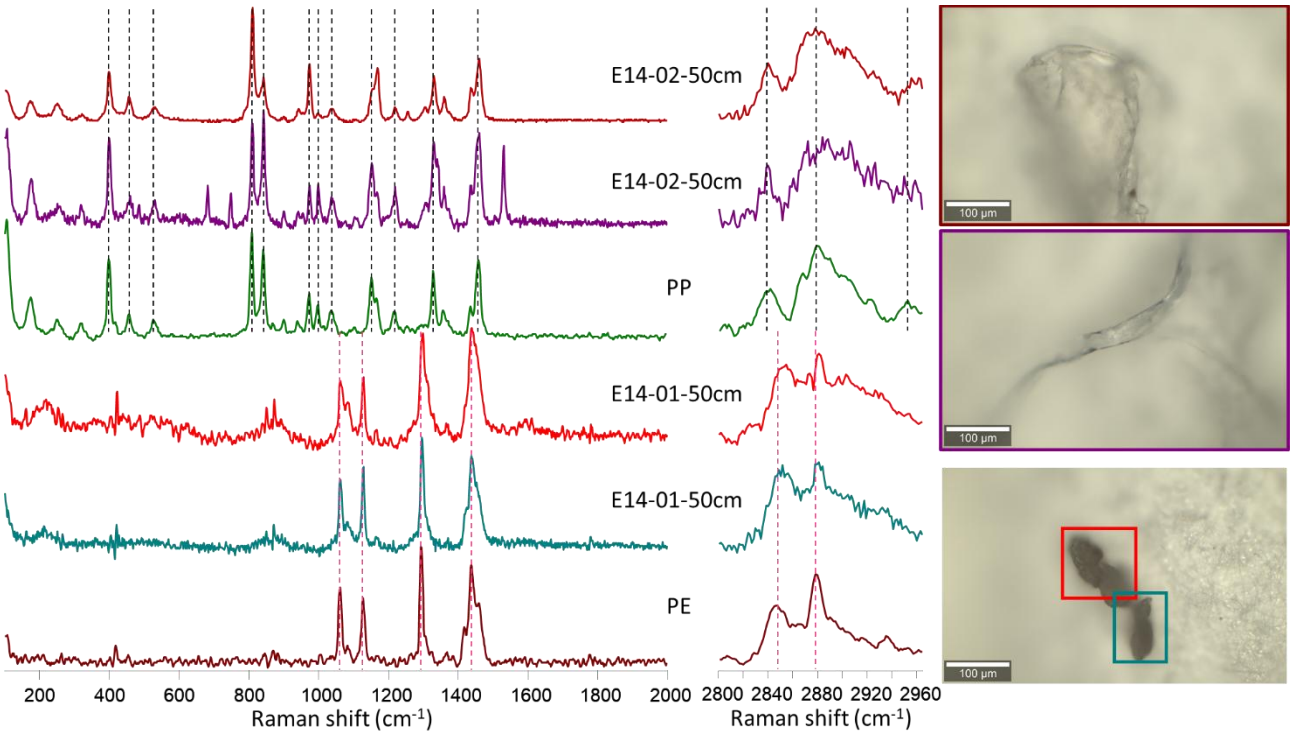

Figure 5. Raman spectra of fibers collected from suspended sediments of E14-Hamburg water sampled at 50 cm depth. The Raman spectra of micronized PP and PE were included as a reference, demonstrating that the particles found are made from these polymers. Particles were visualized on a glass fiber membrane. All spectra were processed by correcting the baseline, removing cosmic rays, and normalizing. Back and magenta dashed lines indicate the peaks assigned to PP and PE, respectively. Bright images show the shape and size of the particles analyzed.

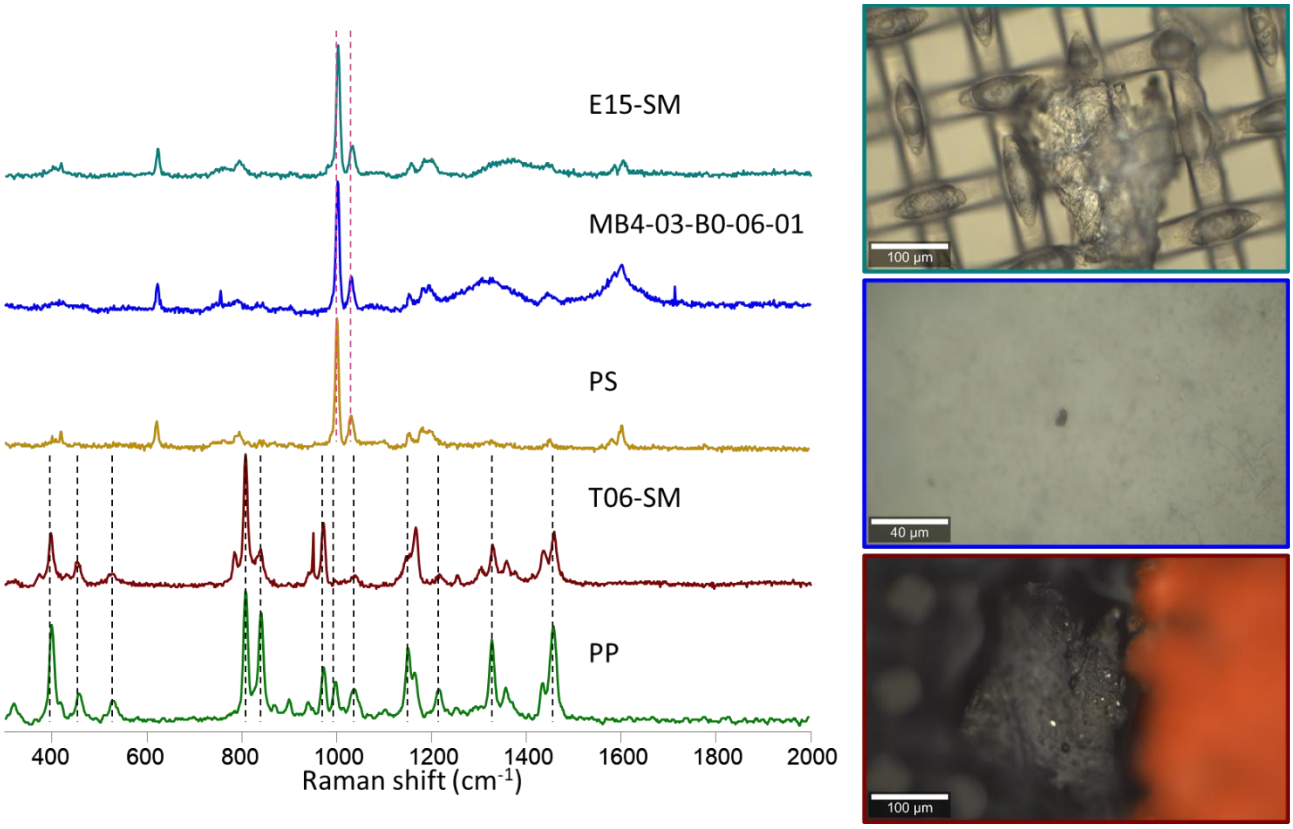

Figure 6. Raman spectra of fibers collected from suspended sediments of E15-Geesthacht and MB4-03-BO-06-01. The Raman spectra of micronized PS and PP were included as a reference, demonstrating that the particles found are made from these polymers. Particles were visualized on a nylon membrane and anodisc. All spectra were processed by correcting the baseline, removing cosmic, and normalizing. Black and magenta dashed lines indicate the peaks assigned to PP and PS, respectively. Bright images show the shape and size of the particles analyzed.

Other particles and fibers were analyzed. Few particles were identified as cellulose/cotton, quartz, and titanium oxide, while a high number of fibers were not identified since they did not display characteristic peaks relative to common-use plastics (data not shown).[7]

3 WATER SAMPLES ANALYSIS

All water samples received at INL were analyzed by NTA to assess the presence of nanoplastics (herein defined as particles with a size below 1 µm[8]). The water samples were filtered with a 1 µm nylon membrane before NTA analysis. Size, size distribution and concentration of particles in the sample (particles/mL) were estimated within the range of 1 µm – 50 nm. The parameters for NTA analysis were selected according to the better visualization of plastics spiked in ultrapure water as reported in our recent publication[9]. The detailed discussion of these results was described in Deliverable 4.3. Figure 7 shows the concentrations of particles below 1 µm estimated for surface microlayer samples from Mero-Barces, Thames, Elbe and North Sea, and water samples from the North Sea collected using CTD and a marine snow catcher. Summarizing; the presence of particles <

[7] Nava V, Frezzotti ML, Leoni B. Raman Spectroscopy for the Analysis of Microplastics in Aquatic Systems. Applied Spectroscopy. 2021;**75**

[8] N. B. Hartmann, T. Hüffer, R. C. Thompson, M. Hassellöv, A. Verschoor, A. E. Daugaard, S. Rist, T. Karlsson, N. Brennholt, M. Cole, M. P. Herrling, M. C. Hess, N. P. Ivleva, A. L. Lusher and M. Wagner, Are We Speaking the Same Language? Recommendations for a Definition and Categorization Framework for Plastic Debris, *Environ. Sci. Technol.*, 2019, **53**, 1039–1047.

[9] Sorasan C, Taladriz-Blanco P, Rodriguez-Lorenzo L, Espiña B, Rosal R. New versus naturally aged greenhouse cover films: Degradation and micro-nanoplastics characterization under sunlight exposure. Science of the Total Environment 2024, **918**.

1 µm in all the water samples analysed seems to be in the range between 10^7 and 10^8 particles/mL and the water thermocline seems to be a barrier for them as the number of particles below the thermocline is always lower than above (see CTD results in Figure 7, higher concentration in the CTD-Top than in CTD-bottom). Additionally, water samples from the winter campaign had higher concentrations of particles smaller than 1 µm than in the summer, independently of the sampling method used and the case study (e.g. Mero-Barces and North Sea).

Taking account the limit of detection (LoD) described for Raman analysis for PET, and PS nanoplastics (D4.2) (5 mg/L for both 161 nm PS and 450 nm PET in freshwater, which correspond to ~ 10^9 particles/mL - ~ 10^8 particles/mL, and 1.25 mg/L = = 4×10^{10} particles/ mL and 0.63 mg/L = 10^7 particles/mL for 36 nm PS and 450 nm PET, respectively) and the highly diverse LoD of the smallest small microplastic using the lab-on-a-chip (0.5 mg/L for PS and PET, but 10 mg/L for PE and PP), we selected the water samples that displayed the highest concentration estimated by NTA (see Figure 7):

- **Mero-Barces**: None of the samples were analysed by Raman or Py-GC-MS analysis. Raman's analysis of any of the samples from Mero-Barcés would be highly hindered, even if all particles detected by NTA were plastics, as LoD concentration cannot be attained.
- **Thames River**: Only one sample was selected: T05-Central London.
- **Elbe River:** Water sampled in E14-Hamburg (downstream of the urbanized area) at 50 and 200 cm in depth, E15-Geesthacht (The tidal limit), E16-Dömitz (industrial and rural influences), and E17-Dessau (industrial and rural influences).
- **North Sea:** Residual water from the marine snow catcher, specifically water collected during the Winter campaign from above the aggregate layer and filtered and unfiltered residual water from the aggregated layer sampled in NS7-Thames estuary, NS9-Broad Fourteens, NS10-West Frisian, and NS12-Elbe estuary. In addition, two water samples from the surface microlayer (NS10-West Frisian, and NS12-Elbe estuary) and one water sample from CTD above the thermocline (NS7-Thames estuary)

Samples were subjected to cloud-point extraction (CPE) to pre-concentrate and eliminate part of the undesirable particulate organic matter and suspended sediments (more details in D4.1). Briefly, 40 mL of the water sample was dispersed in 4 mM Triton-X114 and incubated in pre-boiled water for 1 h. It is worth noting that the volume used for snow catcher samples was smaller, i.e. 10 mL, because stocks of field samples were not more than 30 mL. Then, the supernatant (surfactant-poor phase) was removed using glass Pasteur pipettes, and the pellet (surfactant-rich phase) was re-dispersed in 1 mL of ultrapure water. Finally, this surfactant-rich phase was filtered by a 0.2 µm anodisc and washed using a 4 mL ethanol: water (1:1) mixture. This last step removes the excess Triton, allowing the Raman and Py-GC-MS analysis. This procedure was carried out quadrupled, except with snow catcher samples, which were duplicated. Thus, three independent replicates (one for snow catcher samples) were sent to UDC for Py-GC-MS analysis, and the remaining replicate was analyzed by Raman spectroscopy both directly in the anodisc and inside the lab-on-a-chip system for the smallest small microplastics (see D4.2).

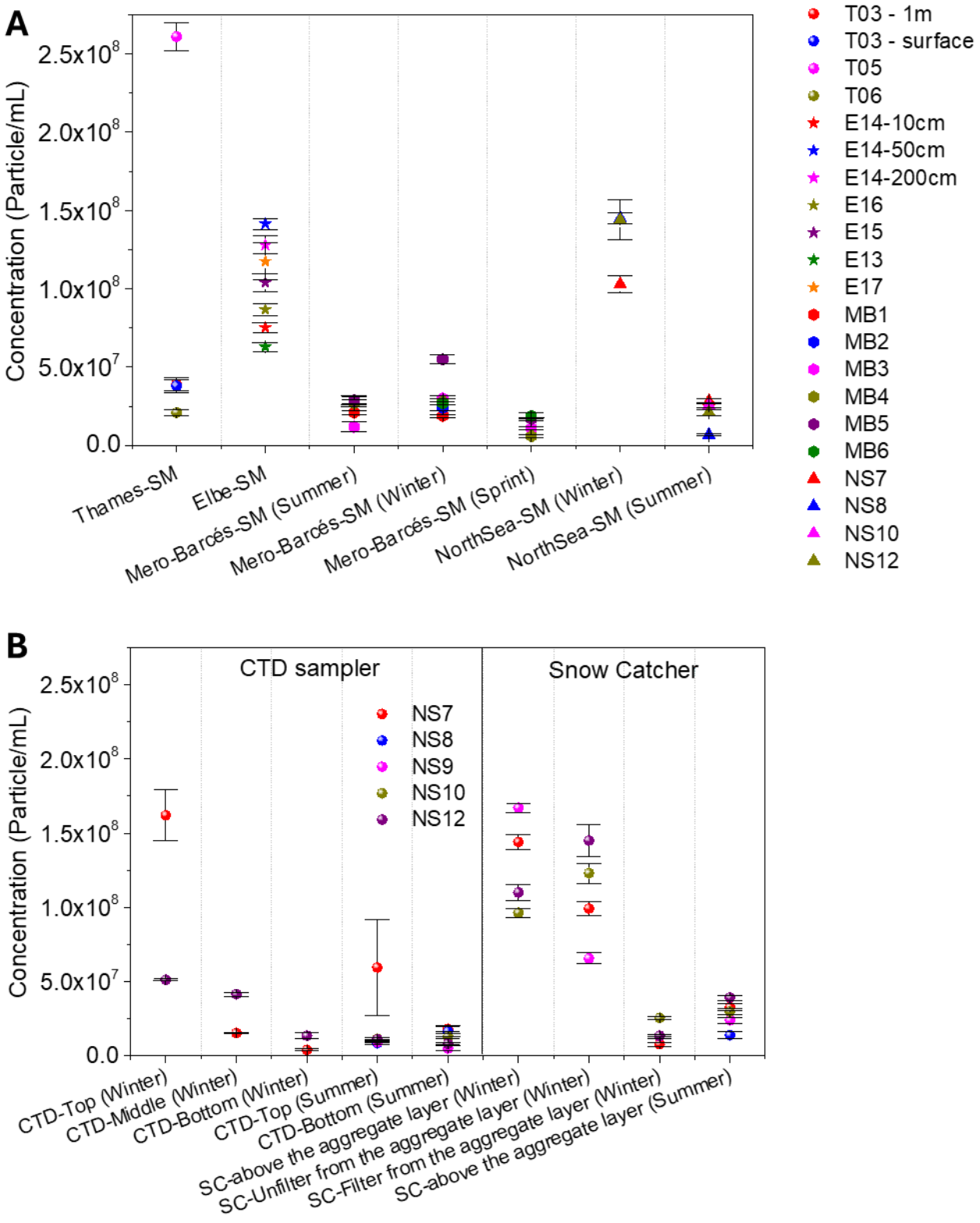

Figure 7. Concentration of particles below 1 µm per millilitre for water samples from Mero-Barces, Thames, Elbe, and North Sea collected using (A) Surface Microlayer collected with a Garrett screen system, (B) CTD and marine snow catcher. T03 and E14 samples were collected using bottles and pump filters, respectively. For the NTA measurements, samples were filtered.

3.1 Py-GC-MS analysis

Pyrolysis gas chromatography-mass spectrometer (Py-GC-MS) is mainly utilized for the chemical identification of macromolecules such as polymers, which cannot be analyzed by either liquid or gas chromatography due to their large size. Briefly, these macromolecules are broken down into simpler molecules through pyrolysis (i.e., controlled thermal degradation). These smaller molecules, i.e., characteristic indicator ions, can then be separated by GC and detected by MS.

Independent replicates of CPE-treated samples were sent to UDC for Py-GC-MS analysis. The CPE procedure was carried out using 40 mL of sample per CPE, except in the case of the samples collected using a snow catcher in the Winter campaign. The volume of water sampled using a marine snow catcher was limited: we had only 30 mL per sample. Therefore, the CPE was performed using only 10 mL and only one replicate. For the rest of the samples, CPE was done in triplicate.

The detailed Py-GC-MS procedures have been described in D3.1, section 5 Microplastics Identification/Quantification, sub-section 5.2 Thermoanalytical methods: Pyrolysis-GC-MS (PY-GC-MS). Briefly, Py-GC-MS measurements are performed with a micro-furnace pyrolyzer EGA/Py-3030D equipped with an autoshot sampler (both Frontier Labs, Japan) attached to an Agilent gas chromatograph with a DB-5MS column coupled to an Agilent MSD mass spectrometer.

To quantify SMNPs correctly by Py-GC-MS, specific indicator compounds must be determined. The most abundant and polymer-specific pyrolysis products were chosen. The calibration was performed by weighing (≈40 µg —1000 µg) directly into pyrolysis cups. Anthracene d10 was added as an internal standard.

Eleven of the most common plastic polymers found in the environment including PS, PET, PE, PP, acrylonitrile butadiene styrene copolymer (ABS), styrene-butadiene rubber (SBR), PMMA, PC, PVC, PA 6 (Nylon-6), and PA 6,6 (Nylon 6,6) were analyzed to determine the characteristic indicator ions (more details D3.1). Styrene trimer, dimethyl terephthalate, 1,16-heptadecadiene, 2,4-dimethylhept-1-ene, 2-phenethyl-4-phenylpent-4-enenitrile, 4-vinylcyclohexene, methyl methacrylate, bisphenol A dimethyl ether, naphthalene, N-methyl caprolactam, and cyclopentanone were selected for PS, PET, PE, PP, ABS, SBR, PMMA, PC, PVC, PA 6, and PA 6,6, respectively. Table 1 and Table 2 summarize the concentrations quantitatively measured by Py-GC-MS for North Sea water samples and Elbe and Thames water samples, respectively. The values obtained could be underestimated due to the recovery rate of CPE being strongly influenced by the size, density and aggregate degree of the plastic particles, being in the range of 10 – 20 % for the smallest particles (≤ 1 µm) and colloidally stable and 60 – 73 % for bigger particles and aggregates (more details D4.1). However, CPE offered a 100 – 200-fold pre-concentration rate, which allowed the detection of SMNPs in Py-GC-MS and microRaman.

Focusing on North Sea samples, PS, PET, PE, ABS, and SBR were not detected in any of the selected samples by Py-GC-MS. PP was identified only in samples collected using a marine snow catcher, mainly in samples related to the water above the aggregated layer: 48.0 µg/L for NS7- Thames estuary, 45.9 µg/L for NS9 – Broad Fourteens, and 86.6 µg/L (Table 1). Other plastic polymers that were not included in the optimization of the sample preparation guideline and Raman identification were detected. Water sampled using a marine snow catcher displayed higher concentrations of plastics than samples collected using CTD or from the surface microlayer (see Table 1). These differences are bigger than we could expect from NTA results, as shown in Figure 7. This difference could be attributed to the size range that NTA can analyze, which is ≤ 1 µm. Therefore, the contribution of bigger particles of 1 µm is not counted in the NTA analysis.

PMMA, PVC, and PA 6 were found in all selected samples from the North Sea. Overall, the highest concentrations found in the samples corresponded to PVC (Table 1). However, these values may suffer a matrix effect, overestimating the concentration of PVC. This is due to naphthalene, the selected indicator ion for PVC, being very unspecific as it can also be generated during the pyrolysis of other synthetic polymers, such as PET or organic substances.[10] The concentration of PA 6 in snow catcher samples seems to present a tendency: higher concentrations in residual water above the aggregate layer than in water from the aggregate layer. Interestingly, the concentration of PA 6 was higher in filtered samples from the aggregate layer than in unfiltered samples, in contrast with the NTA results (the particles' concentration decreased in the filtered samples). This decrease could be because of the increase in aggregation during the filtration process, reducing the number of particles below 1 µm. A similar tendency was observed for PA 6,6 in the NS10- West Frisian, the only sample that contains PA 6,6 in the three types of samples collected using a snow catcher. No evident tendency was observed in the concentrations found in PMMA.

Table 1. Mass concentration (µg/L) of SMNPs in North Sea water samples.

Sample	PyGC-MS											
	PP		PMMA		PC (Polycarbonate)		PVC		PA 6 (Nylon-6)		PA 6,6 (Nylon 6,6)	
	1,4-Dimethylhept-1-ene		Methyl methacrylate		Bisphenol A dimethylether		Naphthalene		N-Methyl caprolactam		Ciclopentanone	
	mean (µg/L)	SD	mean (µg/L)	SD	mean (µg/L)	SD	mean (µg/L)	SD	mean (µg/L)	SD	mean (µg/L)	SD
NS10 SM (Winter)	<LoD		3.117	0.654	0.108	0.063	61.800	8.852	5.050	4.941	<LoD	
NS12 SM (Winter)	<LoD		3.925	1.450	0.050	0.000	58.467	17.170	1.375	2.382	<LoD	
NS7 - CTD Top (Winter)	<LoD		1.500	0.608	<LoD		96.817	1.919	29.917	18.448	24.200	0.742
NS7 Snow catcher - water about the aggregate layer	48.000		9.800		<LoD		417.900		114.3		74.5	
NS7 Snow catcher - filtered water from the aggregate layer	<LoD		12.600		<LoD		374.100		80.3		72.3	
NS7 Snow catcher - unfiltered water from the aggregate layer	40.200		14.200		<LoD		335.900		26.4		<LoD	
NS9 Snow catcher - water about the aggregate layer	45.900		8.5		<LoD		247.200		85		<LoD	
NS9 Snow catcher - filtered water from the aggregate layer	<LoD		7.200		<LoD		282.700		53.1		<LoD	
NS9 Snow catcher - unfiltered water from the aggregate layer	<LoD		4.400		<LoD		223.700		28.8		<LoD	
NS10 Snow catcher - water about the aggregate layer	86.600		22.000		0.200		568.800		582.5		114.600	
NS10 Snow catcher - filtered water from the aggregate layer	<LoD		6.400		<LoD		581.700		198.9		99.400	
NS10 Snow catcher - unfiltered water from the aggregate layer	<LoD		13.000		<LoD		589.200		127.200		72.7	
NS12 Snow catcher - water about the aggregate layer	<LoD		6.200		<LoD		389.600		176.400		<LoD	
NS12 Snow catcher - filtered water from the aggregate layer	<LoD		<LoD		<LoD		314.100		85.400		<LoD	
NS12 Snow catcher - unfiltered water from the aggregate layer	<LoD		7.800		<LoD		199.100		42.400		<LoD	

Analyzing the selected samples from the Elbe and Thame rivers, high variability was observed between replicates of the same water samples, i.e., E17-Dessau, and E14-Hamburg collected at 50 cm depth (Table 2). This could have a significant impact on the sampling protocol for the analysis of SMNPs. Further investigations should be conducted in this field. PE was not detected in any of the samples, while PS and PET were detected in one of the replicates of E14-Hamburg collected at 50 cm depth. However, these plastic polymers were only

[10] Kamp, J., Dierkes, G., Schweyen, P.N., Wick, A., Ternes, T.A., Quantification of Poly(vinyl chloride) Microplastics via Pressurized Liquid Extraction and Combustion Ion Chromatography. Environmental Science & Technology, 2023, **57.**

determined in one of the CPE-treated samples. PP was found in two samples, E17-Dessau and E16-Dömitz, but very high variability in the concentration values was also observed. The highest concentrations were obtained for PVC, as in North Sea samples. PMMA, PC, and PA 6,6 were detected in all samples, except PC in E16-Dömitz.

Table 2. Mass concentration (µg/L) of SMNPs in Elbe River and Thames River water samples.

Sample	PyGC-MS															
	PS		PET		PP		SBR		PMMA		PC		PA 6		PA 6,6		PVC	
	Styrene trimer		Dimethyltere phthalate		1,4-Dimethylhept-1-ene		4-Vinyl cyclohexene		Methyl methacrylate		Bisphenol A dimethylether		N-Methyl caprolactam		Ciclopentanone		Naphthalene	
	mean (µg/L)	SD	mean (µg/L)	SD	mean (µg/L)	SD	mean (µg/L)	SD	mean (µg/L)	SD	mean (µg/L)	SD	mean (µg/L)	SD	mean (µg/L)	SD	mean (µg/L)	SD
E17-01-Dessau	<LoD		<LoD		35.742	61.91	<LoD		4.775	1.724	0.017	0.029	17.058	7.444	19.417	1.509	199.383	72.417
17-02-Dessau	<LoD		<LoD		2.808	4.864	<LoD		12.183	13.395	0.017	0.029	2.333	4.041	<LoD		96.733	3.822
16-01-Dömitz	<LoD		<LoD		3.233	5.6	<LoD		1.667	0.513	<LoD		15.583	7.191	<LoD		54.833	7.363
E14-01-50cm-Hamburg	1.233	2.136	<LoD		<LoD		<LoD		2.683	1.684	0.033	0.029	9.617	11.829	<LoD		123.558	16.464
E14-02-50cm-Hamburg	<LoD		2.067	2.141	<LoD		5.275	9.137	10.483	17.023	0.017	0.029	136.725	2.086	15.075	13.448	545.408	879.438
E14-01-200cm-Hamburg	<LoD		<LoD		<LoD		<LoD		5.375	9.310	0.088	0.018	12.392	2.257	<LoD		208.133	194.791
T05-Central London	<LoD		<LoD		<LoD		<LoD		0.717	1.241	0.025	0.043	8.867	9.042	<LoD		198.867	35.237

3.2 Raman analysis

Raman analysis of anodiscs was performed using the 785 nm laser line and 20x and 50x objectives. The laser power at the sample was ≤ 7 mW. These conditions were optimized for detecting PP, PET, PE, and PP. The detection of other plastics is not guaranteed. On the one hand, many of the localized particles presented strong fluorescence and therefore, the Raman identification was not possible in those cases. On the other hand, particles with different chemical compositions summarise the results of the particles' analysis as follows:

- **E17-Dessau.** PS and PP particles were identified by confocal Raman microscopy as shown in Figure 8. Comparing these results with Py-GC-MS results, a discrepancy was found in the detection of PS since this was identified by Raman, but its presence could not be confirmed by Py-GC-MS (Table 2). PP was found using both techniques.

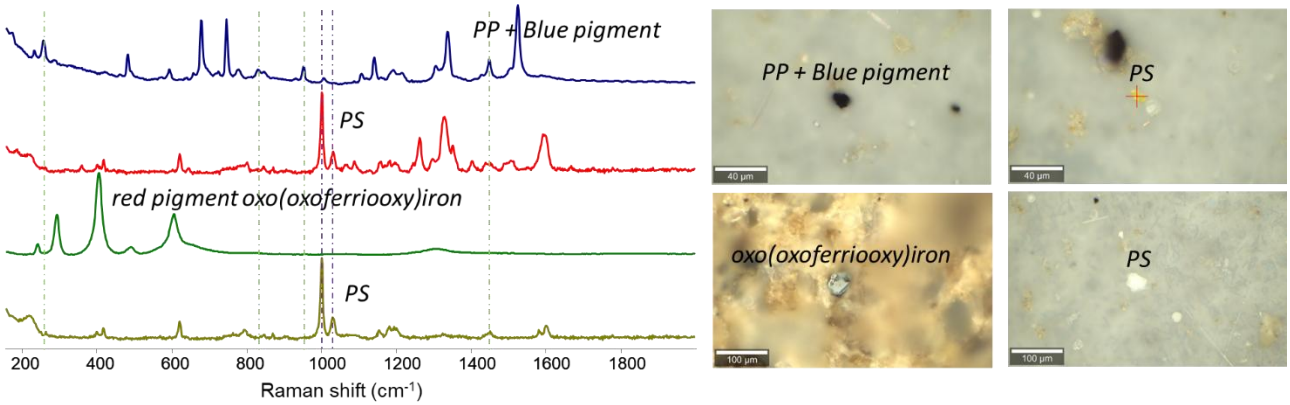

Figure 8. Representative Raman spectra of particles collected from E17-Dessau water after CPE and filtration using a 0.1 µm anodisc. All spectra were processed by correcting the baseline, removing cosmic, and normalizing. Green and purple dashed lines indicate the peaks assigned to PP and PS, respectively. Bright images show the shape and size of the particles analyzed.

- **E14-Hamburg sampled at 50 cm depth (**Figure 9**).** PS and PE were identified, and some characteristic peaks, i.e., 638, 840, and 1450 cm^{-1}, of PVC were assigned to one of the particles. Other types of particles were identified as graphene oxide, amorphous carbon, anatase TiO2, and cellulose. Some Raman spectra could not be assigned to any molecule (see purple spectrum in Figure 9). Both PS and PVC were in relevant amounts by PyGC-MS. However, the presence of PE was not confirmed by PyGC-MS, since the quantity of this plastic is lower than the LoD of the technique (Table 2).

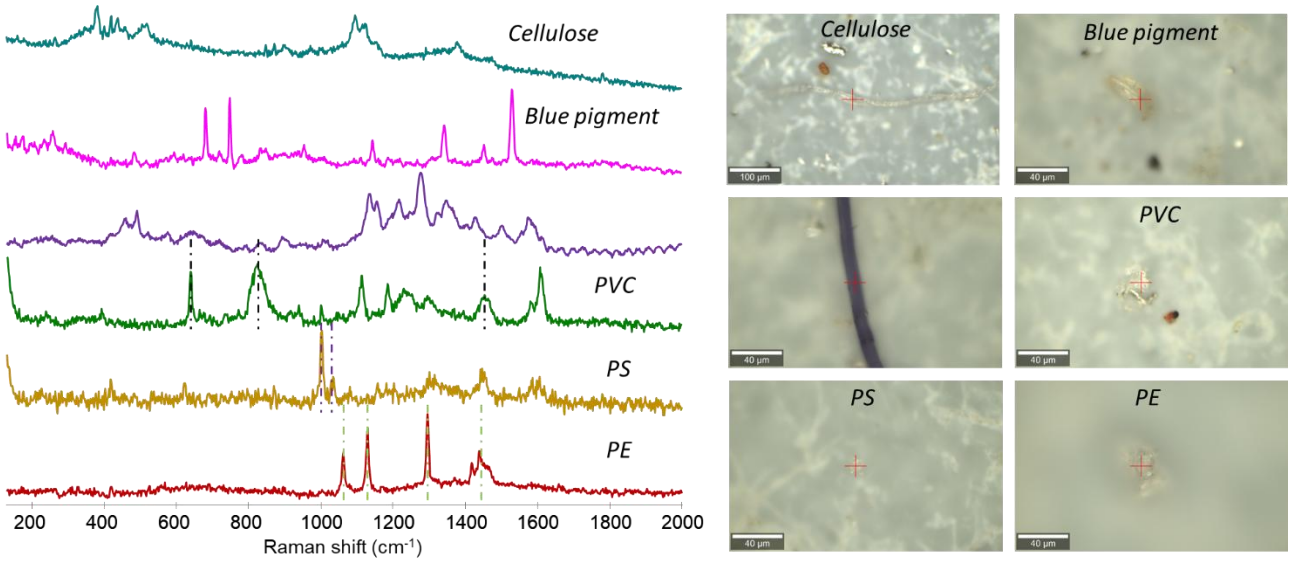

Figure 9. Representative Raman spectra of particles collected from E14-Hamburg water sampled at 50 cm depth after CPE and filtration using a 0.1 µm anodisc. All spectra were processed by correcting the baseline, removing cosmic, and normalizing. Black, Green and purple dashed lines indicate the peaks assigned to PVC, PE and PS, respectively. Bright images show the shape and size of the particles analyzed.

- **E14-Hamburg sampled at 200 cm depth**. No particle was identified as plastic in this sample. Other types of particles were found, such as amorphous carbon, anatase TiO_2, and quartz (data not shown). In general, high fluorescence was observed during particle measurements.
- **E16-Dömizt**. No particle was identified as plastic in this sample. Other types of particles were found, such as amorphous carbon, anatase TiO_2, and cellulose (data not shown).
- **T05-Central London.** No particle was identified as plastic in this sample. Other types of particles were found, such as amorphous carbon and cellulose (data not shown). In general, high fluorescence was observed during particle measurements.
- **North Sea water was sampled using a marine snow catcher.** PS was detected in three different samples: residual water above the aggregate layer and filtered water from the aggregate layer sampled in NS9-Broad Fourteen, and residual water above the aggregate layer sampled in NS10-West Frisian Area. PP was only detected in water above the aggregate layer sampled in NS10-West Frisian Is. No plastic particles were identified in the rest of the snow catcher samples (Figure 10). Comparing these results with Py-GC-MS results, a discrepancy was found in the detection of PS since this was identified by Raman, but its presence could not be confirmed by Py-GC-MS (Table 1). PP was determined by both techniques.

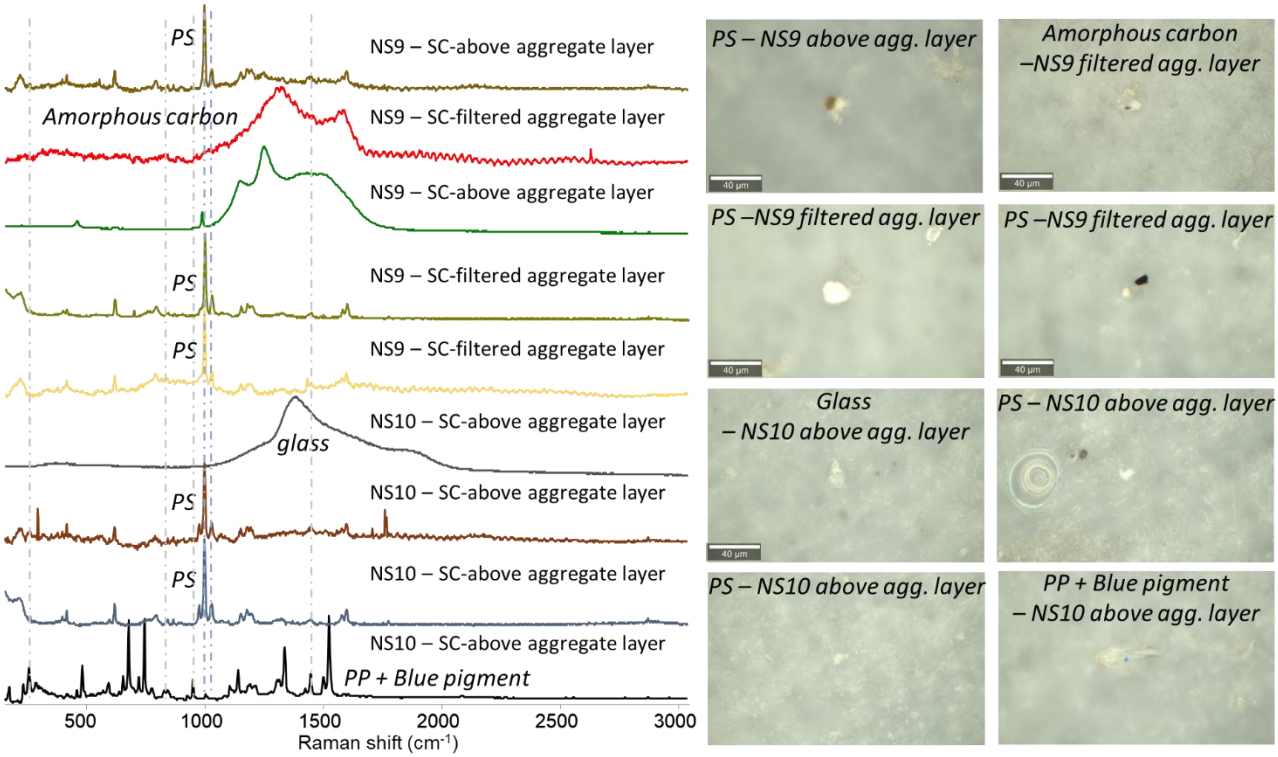

Figure 10. Representative Raman spectra of particles collected from North Sea water sampled using a marine snow catcher after CPE and filtration using a 0.1 µm anodisc. All spectra were processed by correcting the baseline, removing cosmic, and normalizing. Blue and grey dashed lines indicate the peaks assigned to PS and PP, respectively. Bright images show the shape and size of the particles analyzed.

- **Surface microlayer of NS10-West Frisian Is. andNS12–Elbe Estuary.** No particle was identified as plastic in these samples. Other types of particles were found, such as amorphous carbon. In general, high fluorescence was observed during particle measurements.
- **NS7-Thames Estuary – CTD Top.** PP was identified by confocal Raman microscopy as shown in Figure 11. Comparing these results with Py-GC-MS results, a discrepancy was found in the detection of PP since its presence could not be confirmed by Py-GC-MS (Table 1).

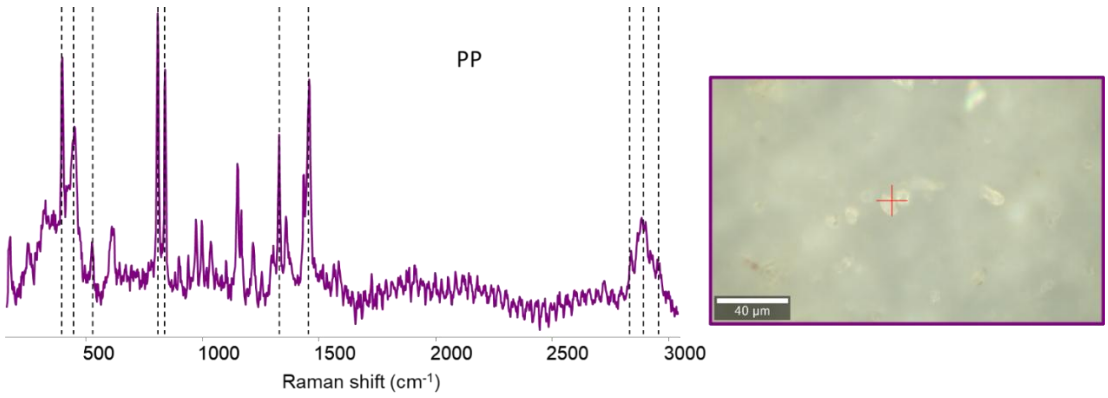

Figure 11. Representative Raman spectrum of a particle collected from NS7-Thames Estuary water sampled using CTD above the thermocline after CPE and filtration using 0.1 µm anodisc. The spectrum was processed by correcting the baseline, removing cosmic, and normalizing. Black dashed lines indicate the peaks assigned to PP. The bright image shows the shape and size of the particle analyzed.

Plastic particles were not identified directly in the anodisc by microRaman in any of the water samples due to either fluorescence interference /or lack of pre-concentration. Therefore, we performed the Raman analysis of the same samples inside the lab-on-a-chip developed in WP4 (see details in D4.2) by resuspending the particles from the anodisc filter and subsequent injection of the suspension. The design of this device is CONFIDENTIAL because the patenting process is ongoing. Raman spectra were acquired using 785 nm laser lines, a 20x objective and a laser power $\geq$ 25 mW. The identification of the plastic was carried out using a Raman library of microplastics (STJ Spectral Databases).

Interestingly, plastic particles were not detected in either NS7-Thames Estuary, sampled using CTD above the thermocline, or E17-Dessau, using the lab-on-a-chip device. It is worth noting that particles smaller than 1 µm cannot be analyzed with these devices. The particles identified as PP and PS had very small sizes (see Figure 8 and Figure 11). Cellulose microparticles were identified in this sample. A similar situation occurred for the NS12–Elbe Estuary surface microlayer sample and the T05-Central London sample, where only cellulose microplastics and glass were detected. In contrast, some microplastics could be identified as PE and polyvinylidene dichloride (PVDC) in the NS10-West Frisian Island surface microlayer, while PS, plastic additives, and copolymers were detected in water above the aggregate layer NS7–Thames Estuary sampled using a snow catcher (Figure 12).

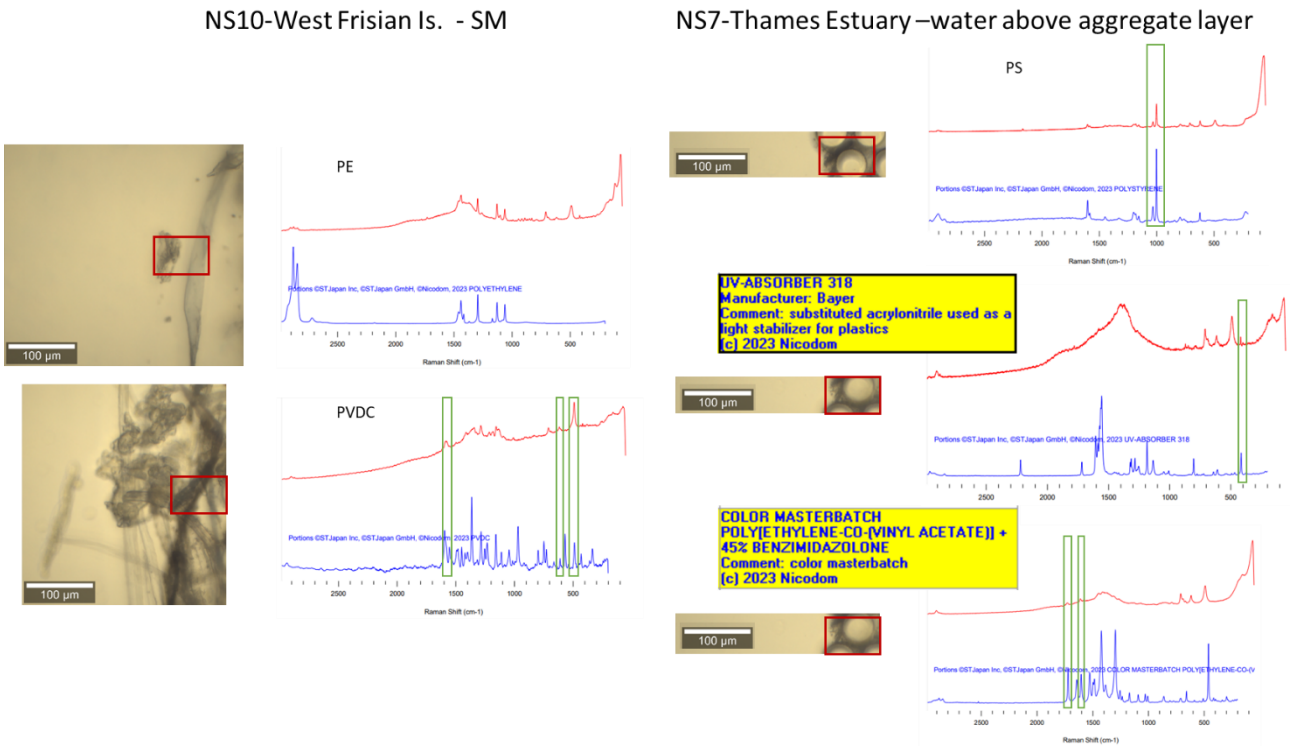

Figure 12. Representative Raman spectra of microplastics detected inside the Lab-on-a-chip. The identification was carried out using a Raman library of microplastics (STJ Spectral Databases).

PE was also detected in E14-Hamburg sampled at 50 cm depth using the lab-on-a-chip device, matching the particle as shown in Figure 9. We could also identify PS in E14-Hamburg sampled at 200 cm depth.

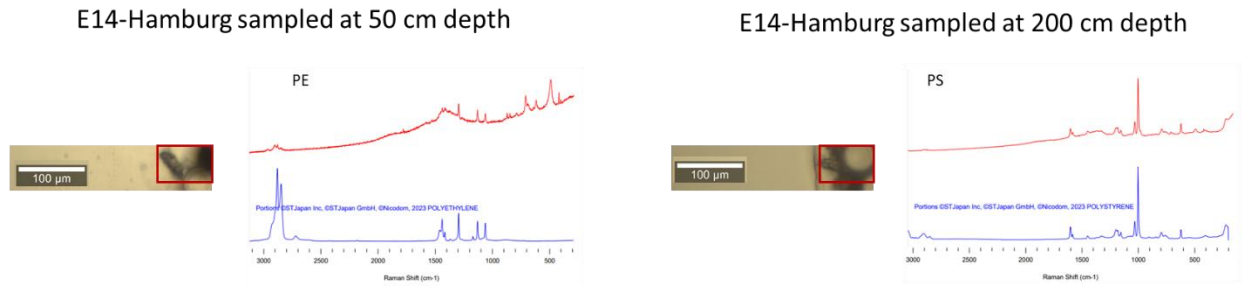

Figure 13. Representative Raman spectra of microplastics detected inside the Lab-on-a-chip. The identification was carried out using a Raman library of microplastics (STJ Spectral Databases).

We identified microplastics in almost all water samples from the North Sea collected using a snow catcher using this lab-on-a-chip device, demonstrating that this device provides the detection of particles at low concentrations, thanks to its high pre-concentration capacity. Figure 14 and 15 show the Raman results obtained. The discrepancies between microRaman and Py-GC-MS remain because PET, PE and PS were identified by Raman, but they could not be confirmed by Py-GC-MS (Table 1. Mass concentration (µg/L) of SMNPs in North Sea water samples.). PVC and PVDC were also possible to be determined, in agreement with Py-GC-MS results.

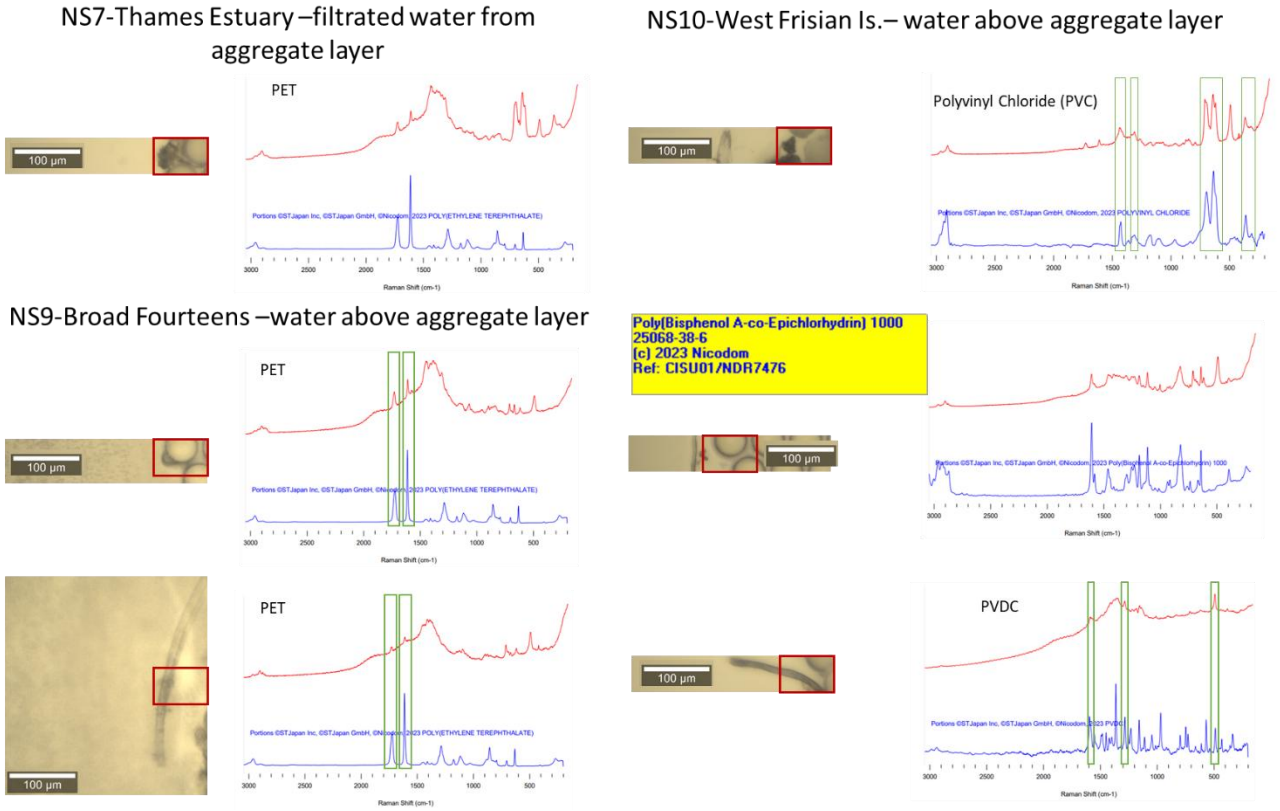

Figure 14. Representative Raman spectra of microplastics found in North Sea samples collected using a marine snow catcher were detected inside the Lab-on-a-chip. The identification was carried out using a Raman library of microplastics (STJ Spectral Databases).

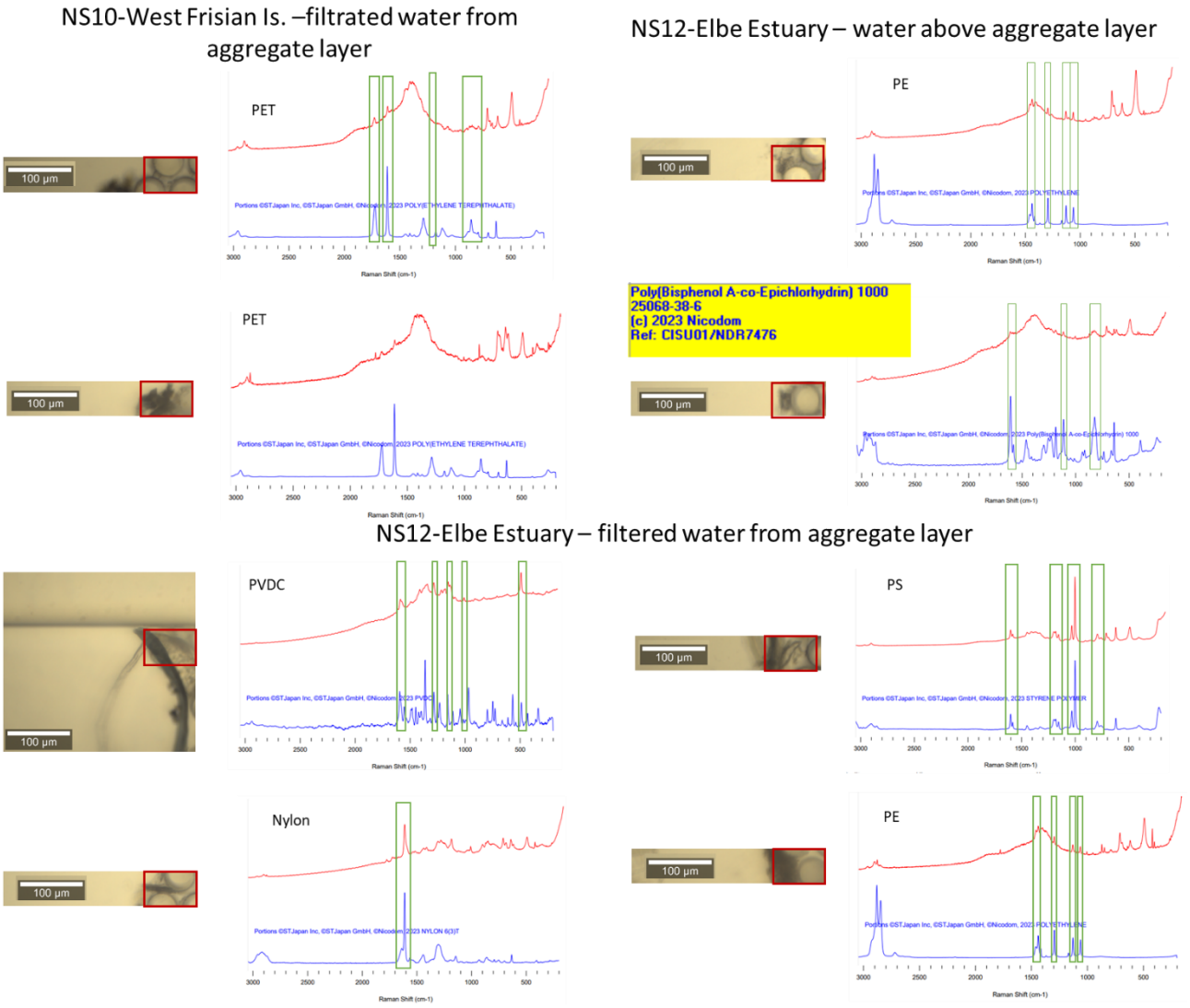

Figure 15. (continuation) Representative Raman spectra of microplastics found in North Sea samples collected using a marine snow catcher were detected inside the Lab-on-a-chip. The identification was carried out using a Raman library of microplastics (STJ Spectral Databases).

GENERAL CONCLUSIONS

The comparison between Raman-based methods and Py-GC-MS allowed gaining a better understanding of the nature and behaviour of SMNPs in suspended sediments and water samples. The presence of additives such as pigments interfered with the DiO staining of particles present in the suspended sediments, which may have an impact on the estimation of the number of SMNPs in the samples. We identified in unstained particles: PP in T03-Windsor water sampled at 1 m, E14-Hamburg at 50 cm depth and T06-Chapman buoy, PE in E14-Hamburg at 50 cm, and PS in E15-Geesthacht and MB4-03-BO-06-01. All particles/fibers had a size in the micro-scale, except the PS particle in MB4-03-BO-06-01, which is close to 1 µm. An automated data analysis pipeline involving pre-processing to eliminate background interference, such as DiO and fluorescence and machine learning and multivariant analysis for the identification of SMNPs will improve the analysis of these particles, reducing uncertainty.

The use of the lab-on-a-chip for the smaller small microplastic allowed the identification of more particles thanks to the reduction of the area of analysis, high preconcentration and decrease of fluorescence interference. However, the implementation of a data analysis pipeline involving pre-processing to eliminate the interference from the material in the microfluidic device, e.g. glass and PDMS, will be needed to establish the use of this tool in the analysis of small microplastics.

Some discrepancies were observed between the results of Py-GC-MS and microRaman. This could be attributed to the analysis principles of each technique. Py-GC-MS quantifies by mass, while microRaman identifies by chemical composition at the single particle level when particles are bigger than 1 µm. For instance, we could detect some PE, PS and PET particles using microRaman. However, most likely the mass of these particles was not sufficient to reach the LoD of Py-GC-MS, particularly in the case of PE. Based on the results, a combination of different analytical techniques is advised to investigate the presence of SMNPs in field samples.

Finally, the lack of reproducibility of the replicates in the quantification by pyrGC-MS indicated that the sampling procedure should be revised for SMNPs analysis. Although the number of particles could be enough to detect their presence in relatively discrete volumes of water after preconcentration, the limitations related to sensitivity depending on mass could postulate the need to establish different requirements of sample volume for Raman or IR and mass spectroscopies.